Estimating Brain Functional Connectivity from Common Subspace Mapping Between Structural and Functional Connectomes

Sanjay Ghosh, Ashish Raj, and Srikantan S. Nagarajan *Fellow, IEEE*

***Abstract*— Understanding the connection between the brain's structural connectivity and its functional connectivity is of immense interest in computational neuroscience. Although some studies have suggested that whole brain functional connectivity is shaped by the underlying structure, the rule by which anatomy constrains brain dynamics remains an open question. In this work, we introduce a computational framework that identifies a joint subspace of eigenmodes for both functional and structural connectomes. We found that a small number of those eigenmodes are sufficient to reconstruct functional connectivity from the structural connectome, thus serving as low-dimensional basis function set. We then develop an algorithm that can estimate the functional eigenspectrum in this joint space from the structural eigenspectrum. By concurrently estimating the joint eigenmodes and the functional eigenspectrum, we can reconstruct a given subject's functional connectivity from their structural connectome. We perform elaborate experiments and demonstrate that the proposed algorithm for estimating function connectivity from the structural connectome using joint space eigenmodes is superior to all other existing benchmark methods.**

***Index Terms*— Brain connectivity, structural connectome, functional connectome, Laplacian, eigen decomposition.**

I. Introduction

The connection between the dynamics of neural processes and the anatomical substrate of the brain is a central question in neuroscience research. Understanding this interplay is essential for understanding how behaviour emerges from the underlying anatomy. To this extent, a common way to represent the whole brain is using a network or graph, where nodes represent cortical and sub–cortical gray matter volumes and edges stand for the strength of structural or functional connectivity. Structural connectivity is typically extracted from tractography algorithms applied to diffusion magnetic resonance imaging (MRI) or diffusion tensor imaging (DTI) data. Functional connectivity usually refers to pairwise correlation between activation signals in various brain regions is measured by various functional brain imaging modalities - functional MRI (fMRI), electroencephalography (EEG), magnetoencephalography (MEG) etc. Although some studies have suggested that whole brain functional connectivity is shaped by the underlying structure, the rule by which anatomy constrains brain dynamics remains an open question. Prior studies offer preliminary evidence that structural networks shape and provide constraints for the dynamics of functional connectivity, which can be measured at different time-scales. However, the exact nature and extent of this relationship is still under-explored. A deeper understanding of how functional connectivity emerges from the structural brain graph is an interesting research challenge [1]. It could help to decouple the activity of brain regions that are not directly connected by structural links. We would then be able to explore how signals propagate between different structural regions, and interfere or interact with each other to induce a global pattern of temporal correlations. Conversely, a fuller understanding of this relationship will allow us to explore that portion of functional activity that are *not* explainable by SC alone; potentially reflecting more complex transynaptic processing across brain network. We build upon the seminal work in [2] that investigated the use of brain connectivity harmonics as a basis to represent spatial patterns of cortical networks. By using the orthogonality of connectome harmonics, it was shown that a linear combination of these eigenmodes can be used to recreate any spatial pattern of neural activity.

Several studies have aimed towards a unified understanding of the mapping between structural and functional connectivity [3]–[8] A broad class of existing literature is built on generative models of functional activity. [1], [3], [9], [10]. The output of these models, with various degrees of complexity, is a simulated functional time–series. The functional connectome is estimated via the correlation of these time–series. A more direct relationship between the structural and functional connectivity matrices have also been considered. Such models aim to directly estimate the functional connectivity from the structural connectivity matrix. No intermediate functional time–series is generated. An emerging approach belonging to this category attempts to find a link between the eigenvalues and eigenvectors of the structural and functional connectivity matrices, and can be referred to as *eigenmode mapping* [5], [11]–[14]. This approach was shown to give accurate prediction of the functional connectome, despite their computational simplicity. A notable study in this category was [12], where authors aimed to predict the functional connectome using the eigenmodes of structural Laplacian. In particular, an exponential curve fitting rule was proposed to estimate the projections of functional connectome (on the eigenmodes of structural Laplacian) from the eigenvalues of the Laplacian. Similarly, authors in [14] posed this structure function mapping as a L_2 minimization

Department of Radiology and Biomedical Imaging, University of California San Francisco, CA 94143, USA.

Corresponding authors: sri@ucsf.edu; ashish.raj@ucsf.edu. Drs. Raj and Nagarajan contributed equally to this work.

problem. However, similar to [12], the feasible eigenmodes were restricted to the individual eigenmodes of structural connectome (roughly equivalent to Laplacian eigenmodes). Despite the success of this approach, it can be limiting to enforce the functional eigenmodes to belong to the space of the structural Laplacian eigenmodes. Further, it was shown by Abdelnour et al. [12] that the one-to-one relationship between the two is only strong at the group average level, and less so at the individual subject level. Recently Becker et al. [13] allowed a more flexible eigenmode mapping, by introducing a rotation matrix along with the structural eigenmodes as a means to capture individual subjects' FC. Their approach to eigenmode mapping was also more advanced and versatile, consisting of a series expansion, achieved via a polynomial fit of the two matrices' eigenvalues.

Regardless of their mutual differences, all above mentioned eigenmode mapping methods rely on constructing independent eigenspectra of both functional connectivity and structural connectivity. In this paper, we introduce a new approach to integrate both structural Laplacian and functional connectivity by a common vector space shared by both the connectomes. Thus, the two matrices' eigenmodes are computed not independently but jointly, using an algorithm based on manifold optimization. This framework allows us to express functional connectivity of a particular subject (brain sample) as a subspace of the joint eigenmodes of structure and function. Notably, just a small fraction of the proposed joint eigenmodes are sufficient to span the functional connectivity. We further extend the core idea to develop a predictive model that is able to accurately predict functional connectivity from structural Laplacian. The bottleneck for this prediction model is to find a mapping from the projection of structural Laplacian and functional connectome to the joint space. We circumvent this by using a nonlinear and data-driven mapping technique. The main contribution in this paper is a state-of-the-art method for structure-function mapping of human brain connectivity.

This paper is outlined as follows. In Section II, we introduce our framework governing the relationship between structural Laplacian and functional connectivity. The details on structure-function predictive model are presented in Section III. Thorough experimental analysis of our approach including state-of-the-art comparisons are contained in Section IV. Finally, we conclude in Section V with a summary of our work.

II. Theory and Methods

Suppose $\boldsymbol{S} \in \mathbb{R}^{N\times N}$ and $\boldsymbol{F} \in \mathbb{R}^{N\times N}$ are the structural and functional connectivity matrices of an arbitrary subject. Here N corresponds to the number of regions-of-interest (ROI) in a brain atlas. The entry (i, j) of these matrices represents the strength of the connectivity between regions i and j evaluated either structurally or functionally.

We consider the problem of finding a joint or common vector space between $\boldsymbol{S}$ and $\boldsymbol{F}$. In other words, our goal is to find a matrix $\mathcal{A} = [\boldsymbol{a}_1|\boldsymbol{a}_2|\ldots|\boldsymbol{a}_N]$ and $\boldsymbol{a}_i \in \mathbb{R}^{N\times 1}, \forall i = \{1, 2, \ldots, N\}$ that can express both structural and functional connectivity by its orthonormal column vectors $\boldsymbol{a}_i$. Without loss of generality, we instead work with the Laplacian of the structural connectivity as in [12]. Let $\boldsymbol{D}$ is the (diagonal) degree matrix of structural connectivity $\boldsymbol{S}$. Then, the (normalized) Laplacian of the structural connectivity is given by:

$$\boldsymbol{L} = (\boldsymbol{I} - \boldsymbol{D}^{-1/2}\boldsymbol{S}\boldsymbol{D}^{-1/2}),$$

where $\boldsymbol{I} \in \mathbb{R}^{N\times N}$ is an identity matrix. Finally, the revised mathematical problem is to find a matrix $\mathcal{A} = [\boldsymbol{a}_1|\boldsymbol{a}_2|\ldots\boldsymbol{a}_N]$ such that:

$$\begin{aligned} \boldsymbol{L} =& \mathcal{A}\Delta_\Phi\mathcal{A}^T \\ \boldsymbol{F} =& \mathcal{A}\Delta_\Psi\mathcal{A}^T. \end{aligned} \tag{1}$$

The above joint diagonalization gives us the pair of diagonal matrices Δ_Φ and Δ_Ψ, where the diagonals $\Phi = \{\phi_1, \phi_2, \ldots, \phi_N\}$ and $\Psi = \{\psi_1, \psi_2, \ldots, \psi_N\}$ constitute the joint eigenspectra of $\boldsymbol{L}$ and $\boldsymbol{F}$ respectively. From the perspective of projection theory, the eigenspectra Φ and Ψ could be viewed as the projections of structural Laplacian and functional connectome on the space spanned by $\{\boldsymbol{a}_1, \boldsymbol{a}_2, \ldots, \boldsymbol{a}_N\}$. For example, ϕ_1 and ψ_1 are the projections of $\boldsymbol{L}$ and $\boldsymbol{F}$ respectively on $\boldsymbol{a}_1$. Thus, the problem in (1) could be equivalently formulated as a minimization as follows:

$$\begin{aligned} \{\mathcal{A}^*, \Phi^*, \Psi^*\} =& \arg\min_{\mathcal{A},\Phi,\Psi} ||\boldsymbol{F} - \mathcal{A}\Delta_\Psi\mathcal{A}^T||_F \\ & \text{s.t. } \boldsymbol{L} = \mathcal{A}\Delta_\Phi\mathcal{A}^T. \end{aligned} \tag{2}$$

The mathematical problem in (2) is a particular case of joint diagonalization, which is a well-studied area in signal processing [16]–[18]. There exist several algorithms to solve (2); here we choose the method by [16] due to its computational simplicity. We refer the columns of $\mathcal{A}$ as joint eigenmodes of the pair $(\boldsymbol{L}, \boldsymbol{F})$. One attractive aspect of joint eigenmodes is that we can diagonalize both structural (Laplacian) and functional connectivity using the same set of these eigenmodes. We note that there is no clear relationship between these joint eigenmodes and individual eigenmodes of structural Laplacian or functional connectivity (connectome). Suppose $(\boldsymbol{U}, \Delta_\Lambda)$ are the eigenmode and eigenspectrum respectively of structural Laplacian $\boldsymbol{L}$ and $(\boldsymbol{V}, \Delta_\Gamma)$ are the eigenmode and eigenspectrum respectively of functional connectome. Then,

$$\boldsymbol{L}\boldsymbol{U} = \boldsymbol{U}\Delta_\Lambda, \boldsymbol{F}\boldsymbol{V} = \boldsymbol{V}\Delta_\Gamma. \tag{3}$$

We note that the dominant eigenmodes of Laplacian $\boldsymbol{L}$ are those eigenvectors with least eigenvalues, whereas dominant eigenmodes of functional connectome $\boldsymbol{F}$ are those eigenvectors with highest eigenvalues.

Suppose the eigenvalues of $\boldsymbol{L}$ are arranged as follows: $\lambda_1 \leq \lambda_2 \leq \ldots \leq \lambda_N$. Then one can show that $0 \leq \lambda_i \leq 2$. A detailed proof is quite straightforward by using two facts: (i) symmetric nature of structural connnectome S and (ii) non-negativeness of each entry of S. We also note that functional connectomes are positive semi-definite matrices because they arise from covariance matrices. Therefore, the eigenvalues in (3) of each functional connectome follows: $\gamma_i \geq 0, \ \forall i$, where γ_i are the diagonal entries of Δ_Γ.

It remains an open question to explore the connections between the joint eigenspectra and individual eigenspectra. We state some interesting theorems on the properties of joint eigenspectra Φ and Ψ as follows:

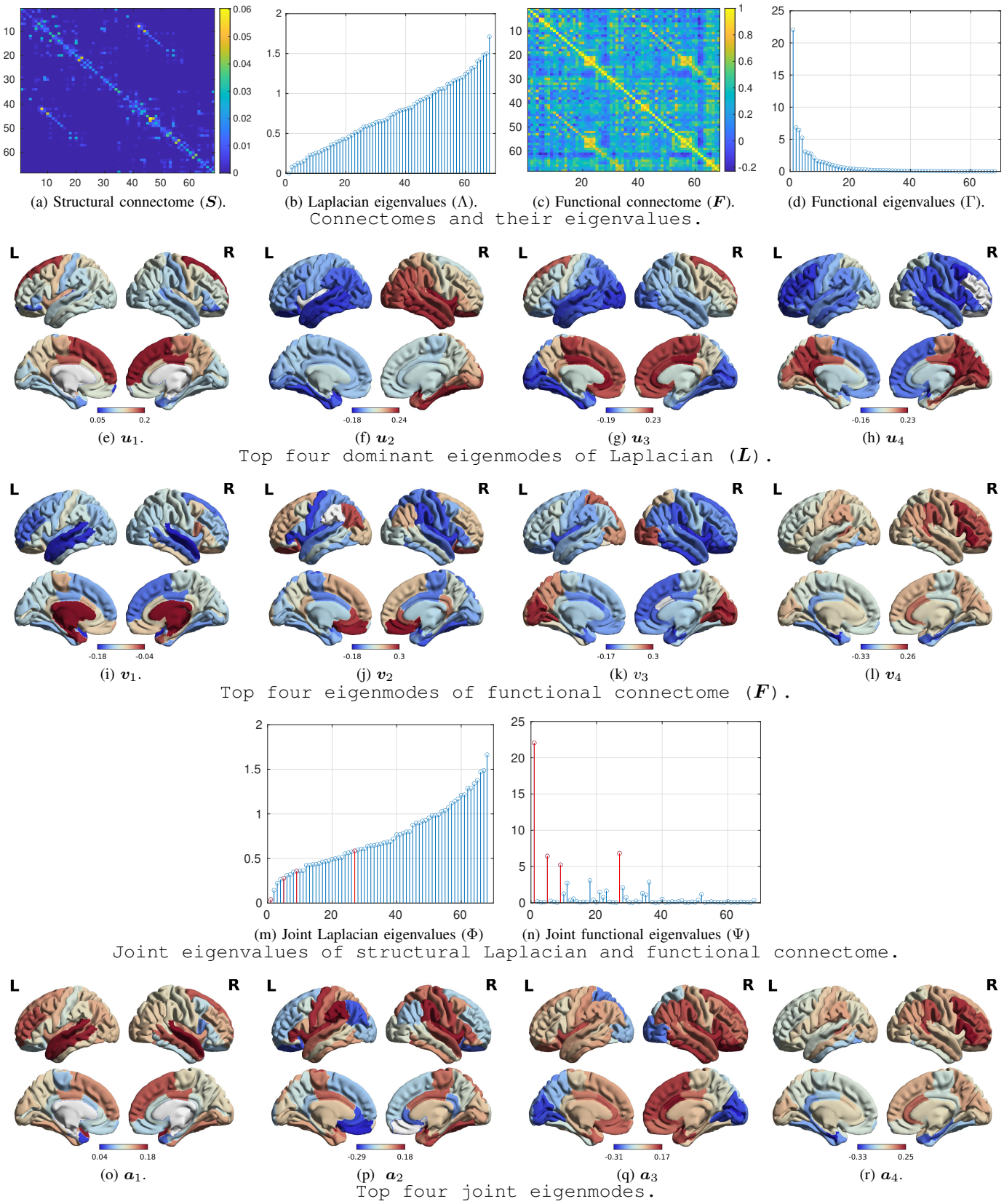

(a) Structural connectome ($\boldsymbol{S}$). (b) Laplacian eigenvalues (Λ). (c) Functional connectome ($\boldsymbol{F}$). (d) Functional eigenvalues (Γ).

Connectomes and their eigenvalues.

(e) $\boldsymbol{u}_1$. (f) $\boldsymbol{u}_2$ (g) $\boldsymbol{u}_3$ (h) $\boldsymbol{u}_4$

Top four dominant eigenmodes of Laplacian ($\boldsymbol{L}$).

(i) $\boldsymbol{v}_1$. (j) $\boldsymbol{v}_2$ (k) v_3 (l) $\boldsymbol{v}_4$

Top four eigenmodes of functional connectome ($\boldsymbol{F}$).

(m) Joint Laplacian eigenvalues (Φ) (n) Joint functional eigenvalues (Ψ)

Joint eigenvalues of structural Laplacian and functional connectome.

(o) $\boldsymbol{a}_1$. (p) $\boldsymbol{a}_2$ (q) $\boldsymbol{a}_3$ (r) $\boldsymbol{a}_4$.

Top four joint eigenmodes.

Fig. 1. A pair of structural and functional connectomes (from public dataset [15]) and their eigenspectra. The line plot in (b) shows eigenvalues of Laplacian of the structural connectome shown in (a). Similarly, the line plot in (d) displays eigenvalues of the functional connectome in (c). In second row, we show the top four eigenmodes (eigenvectors corresponding to least eigenvalues) of the structural Laplacian. Similarly, we show the top eigenmodes of functional connectome in third row. The stem plots in fourth row show the projections of structural Laplacian and functional connectome on the joint eigenmodes. In the buttom row we display top four dominant (with respect to $\boldsymbol{\Psi}$) joint eigenmodes.

Theorem 1: The joint eigenvalues of structural Laplacian $\{\phi_1, \phi_2, \ldots, \phi_N\}$ are bounded:

$$0 \leq \phi_i \leq 2, \quad \forall i \in 1, 2, \ldots, N.$$

Proof: See Appendix A.

Theorem 2: The joint eigenvalues of functional connectome $\{\psi_1, \psi_2, \ldots, \psi_N\}$ are non-negative.

$$\psi_i \geq 0.$$

Proof: See Appendix B.

In Figure 1, for a representative subject, we display a pair of structural and functional connectomes and their respective eigenspectra (ordered). It can be seen that the eigenvalues of $\boldsymbol{L}$ lie in the range $[0, 2]$ and the eigenvalues of the functional connectome are non-negative. The structural and functional eigenmodes corresponding to the dominant/top four eigenvalues $\boldsymbol{L}$ and $\boldsymbol{F}$ respectively are shown in second and third rows of Figure 1. The bottom two rows show the joint eigenspectra, and the top four joint eigenmodes as a result of joint optimization of the $\boldsymbol{L}$ and $\boldsymbol{F}$ pair. We note that there is no visually evident similarity or connection between the joint eigenmodes with the respective dominant (individual) eigenmodes of structural and functional connectomes.

Figure 2 shows (Φ, Ψ) eigenspectra for two other representative subjects. The joint diagonalization is performed independently on $(\boldsymbol{L}, \boldsymbol{F})$ pair for each subject. Notice that eigenvalues in Ψ for each subject *sparse* in nature, most of the eigenvalues are close to zero except a few. This unique nature of the Ψ motivates us to establish a subspace relationship between vector space of structural Laplacian connectome and vector space of functional connectome of the same subject. We note that the most dominant eigenmode is always one corresponds to the least value of Φ. However, subsequent (after the top one) dominant joint eigenmodes do not follow any consistent sequence across subjects.

Subspace Relationship

In this section, we establish that the functional connectome can be reconstructed using only a small number of the joint eigenmodes - i.e. a low-rank subspace. As an example, we re-arrange the joint eigenmodes $\{\boldsymbol{a}_i\}$ $\forall i \in 1, 2, \ldots, N$ and Ψ of the subject from Fig. 1(n) in ascending order of the latter and shown in Fig. 3(a). We plot Pearson R correlation between ground-truth functional connectome and the estimated one from the reduced eigenmodes as a function of number of joint modes (k). Here $k = 1$ implies the estimated functional connectome from only one joint mode and $k = N$ is when all modes are used in the estimation which results in perfect recovery.

Using the properties of SVD, the structural Laplacian can be expressed as outer-products of the joint eigenmodes:

$$\boldsymbol{L} = \sum_{k=1}^{N} \phi_k \boldsymbol{a}_k \boldsymbol{a}_k^T.$$

Similarly, the functional connectome can be expressed as the outer-products of the joint eigenmodes. The Pearson R plot in Fig. 3(b) suggests that $K = 20$ is enough to approximate $\boldsymbol{F}$. In particular:

$$\boldsymbol{F} \approxeq \sum_{k=1}^{K} \psi_k \boldsymbol{a}_k \boldsymbol{a}_k^T.$$

Only a few number ($K \ll N$) of joint eigenmodes sufficiently span the functional connectome. Another example is shown the last row in Figure 3. Here only $K = 30$ dominant modes span the functional connectome ($N = 219$). In summary, the existence of joint eigenmodes and the *sparse* nature of Ψ lead to this subspace relationship. Note that the low-rank nature of functional connectome is also preserved in form of joint subspace [12], [19].

III. Structure-Function Mapping

In this section, we extend the concept of joint eigenspace to estimate functional connectivity of a subject from its structural (via Laplacian) counterpart. Given the joint eigenmodes between the structural Laplacian and functional connectome, the task boils down to estimating Ψ from Φ at an individual subject level. It was reported in [12] that there could be an inverse relationship between $\log(\Psi)$ and Φ based on a linear graph model predicting a subject's functional connectivity matrix from their structural connectivity matrix via graph diffusion [19]. Motivated by the findings in [12], here we aim to estimate Ψ from Φ.

Joint Eigenspectrum Mapping

We propose a data-driven approach to learn a group level mapping between Φ and Ψ. The idea is to consider the diagonals of both Δ_Φ and Δ_Ψ as two points in a vector space of size $\mathbb{R}^{N \times 1}$. Then we pose the mapping between Φ and Ψ as a least-squares problem [20]. Suppose there are M subjects in the group from which learn the least-squares mappings. Therefore, for each subject $j \in \{1, 2, \ldots, M\}$ there is a pair of joint eigenvalues (Φ_j, Ψ_j) obtained by via performing joint diagonalization of the pair $(\boldsymbol{L}_j, \boldsymbol{F}_j)$. First, we embed joint eigenvalues of each subject in two matrices $X \in \mathbb{R}^{N \times M}$ and $Y \in \mathbb{R}^{N \times M}$ as follows:

$$\begin{aligned} X &= [\Phi_1, \Phi_2, \ldots, \Phi_M], \\ Y &= [\Psi_1, \Psi_2, \ldots, \Psi_M], \end{aligned} \tag{4}$$

where $\Phi_j, \Psi_j \in \mathbb{R}^{N \times 1}, \forall j \in \{1, 2, \ldots, M\}$. We consider the following linear transformation $W \in \mathbb{R}^{N \times N}$:

$$Y = WX. \tag{5}$$

To circumvent the limitation of over-fitting incurred by simple least-squares solution, we seek to impose rank constraint [21] on W. Note that this problem is a NP-hard. Various approaches have been proposed in the literature to solve this problem approximately [22]. One efficient approach is to regularize the objective by trace norm (sum of singular values), which is popularly called as nuclear norm. In particular, we consider the following minimization:

$$W = \underset{W}{\text{argmin}} \; ||Y - WX||_F^2 + \mu ||W||_*, \tag{6}$$

where $\mu > 0$ and $||W||_*$ is the nuclear norm of W. We solve the minimization using a primal gradient method [21].

Predicting Functional Connectome with Joint Mapping

Here we aim to estimate the functional connectome $\hat{F}_l$ for an individual subject l, given their structural Laplacian L_l, group level joint eigenmodes and individual joint eigenspectra. An optimal spectrum mapping in (6) would work best under the assumption that joint eigenmodes for each subject is known to us. However, this is not really a realistic assumption from the perspective of a predictive model. We empirically notice that each subject has different set of joint eigenmodes. This is what makes the above formulation as bottleneck to being an efficient predictive model from structural to functional connectome. Instead, our aim is to find a set of group-level joint eigenmodes $\mathcal{A} \in \mathbb{R}^{N\times N}$, where each column represents group-level joint eigenvector. In particular, we consider the following optimization problem:

$$\begin{aligned} \underset{\mathcal{A}}{\text{minimize}} \ \sum_{j=1}^{M} ||\boldsymbol{F}_j - \mathcal{A}\Delta_{\Psi_j}\mathcal{A}^T||_F^2 \\ \text{subject to } \boldsymbol{L}_j = \mathcal{A}\Delta_{\Phi_j}\mathcal{A}^T; \mathcal{A}^T\mathcal{A} = \mathcal{A}\mathcal{A}^T = \boldsymbol{I}, \end{aligned} \tag{7}$$

where $\boldsymbol{F}_j$ and $\boldsymbol{L}_j$ stand for functional connectome and structural Laplacian of subject j respectively. Using eigen spectrum mapping from (5), we get $\Psi_j = W\Phi_j$ which implicitly takes into account the fact that $\boldsymbol{L}_j = \mathcal{A}\Phi_j\mathcal{A}^T$. Further, by using standard trace equality and the connection between Frobenius norm and trace of a matrix, we further simplify the objective function above as follows:

$$\begin{aligned} \sum_{j=1}^{M} \Big(&\text{tr}(\boldsymbol{F}_j^T\boldsymbol{F}_j) - 2\ \text{tr}\big((\boldsymbol{F}_j^T\mathcal{A}\Delta_{W\Phi_j}\mathcal{A}^T\big) \\ &+ \text{tr}\big\{\big(\mathcal{A}\Delta_{W\Phi_j}\mathcal{A}^T\big)^T\big(\mathcal{A}\Delta_{W\Phi_j}\mathcal{A}^T\big)\big\}\Big). \end{aligned}$$

By using $\mathcal{A}^T\mathcal{A} = \boldsymbol{I}$ and cyclic property of trace of matrix, the third term above is simplified to $\big(\Phi_j^T W^T W \Phi_j\big)$. In fact, it is clear that both first and third terms above do not depend on $\mathcal{A}$. Thus, the reduced optimization is:

$$\begin{aligned} \underset{\mathcal{A}}{\text{minimize}} \ -\text{tr}\sum_{j=1}^{M} \boldsymbol{F}_j^T\mathcal{A}\Delta_{W\Phi_j}\mathcal{A}^T \\ \text{subject to } \mathcal{A}^T\mathcal{A} = \mathcal{A}\mathcal{A}^T = \boldsymbol{I}. \end{aligned} \tag{8}$$

It is worth noting that there is no known closed-form solution to (8). We adopt the iterative algorithm described in [23] to find an approximate solution.

In summary, we propose a two-step strategy for the structure function mapping. First, we construct matrices X and Y using both structure and function connectomes of the subjects; then we learn the spectrum mapping W in (6). Second, we solve (8) to obtain group level joint eigenmodes A. In the next iteration, we re-train the mapping W in (5) using these joint eigenmodes followed by estimating a refined group joint eigenmodes using the new mapping. Upon convergence, we obtain a final set of joint eigenmodes $\mathcal{A}$ and spectrum mapping W. We refer the proposed predictive method as *joint eigen spectrum mapping* (JESM).

Detailed steps of the proposed JESM Algorithm are described in 1. We finally obtain the group level joint eigenmodes $\mathcal{A}$ and mapping W, and estimate functional connectome for an arbitrary subject l as follows:

Algorithm 1: Joint Eigen Spectrum Mapping (JESM)

Input: Structural and functional connectomes: $\boldsymbol{S}_j$, $\boldsymbol{F}_j$ for $j \in \{1, 2, \ldots, M\}$.
Output: Joint eigenmodes $\mathcal{A}$ and mapping W.

for $j = 1, 2, \ldots, M$ **do**
  Compute structural Laplacian $\boldsymbol{L}_j$ from $\boldsymbol{S}_j$.
  Perform joint diagonalization of $(\boldsymbol{L}_j, \boldsymbol{F}_j)$ to obtain joint eigenvalues Φ_j and Ψ_j as in (2).
  Embed vectorized joint eigenvaules Φ_j and Ψ_j in matrices X and Y as in (4).
  Obtain spectrum mapping W using (6).
end
Initialize $k \leftarrow 1$
repeat
  Calculate joint eigenmodes $\mathcal{A}$ using (8).
  Recompute joint eigenvelaues: $\Phi_j = \text{diag}(\mathcal{A}^T\boldsymbol{L}_j A)$ and $\Psi_j = \text{diag}(\mathcal{A}^T\boldsymbol{F}_j\mathcal{A})$.
  Embed vectorized joint eigenvaules Φ_j and Ψ_j in matrices X and Y as in (4).
  Obtain spectrum mapping W using (6).
  $k \leftarrow k + 1$.
until *stopping condition is satisfied:* $k = k_{max}$.

$$\begin{aligned} \hat{\Phi}_l &= \text{diag}(\mathcal{A}^T\boldsymbol{L}_l\mathcal{A}). \\ \hat{\Psi}_l &= W\Phi_l. \\ \hat{\boldsymbol{F}}_l &= \mathcal{A}\Delta_{\hat{\Psi}_l}\mathcal{A}^T. \end{aligned} \tag{9}$$

A. Dataset

To validate the proposed brain connectivity analysis framework, we experimented on data from 70 healthy subjects [15]. The brain data acquisition comprised of (i) a magnetization-prepared rapid acquisition gradient echo (MPRAGE) sequence sensitive to white/gray matter contrast, (ii) a DSI sequence (128 diffusion-weighted volumes), and (iii) a gradient echo EPI sequence sensitive to BOLD contrast. These data was pre-processed using the Connectome Mapper pipeline [24]. Gray and white matter were segmented using Freesurfer and parcellated into 83 cortical and subcortical areas. The parcels were then further subdivided into 129, 234, 463 and 1015 approximately equally sized parcels. Structural connectivity matrices are estimated for each subject using deterministic streamline tractography on reconstructed DSI data [25]. Functional data were estimated using the protocol in [26]. This includes regression of white matter, cerebrospinal fluid, motion deblurring and lowpass filtering of BOLD signal.

B. Benchmark Comparisons

We compare the performance of JESM with the following benchmark methods in terms of estimating functional connectivity of a subject from its structural counterpart.

1) Abdelnour et al. [12]: The standalone eigenmodes of structural Laplacian Λ were used to estimate the functional

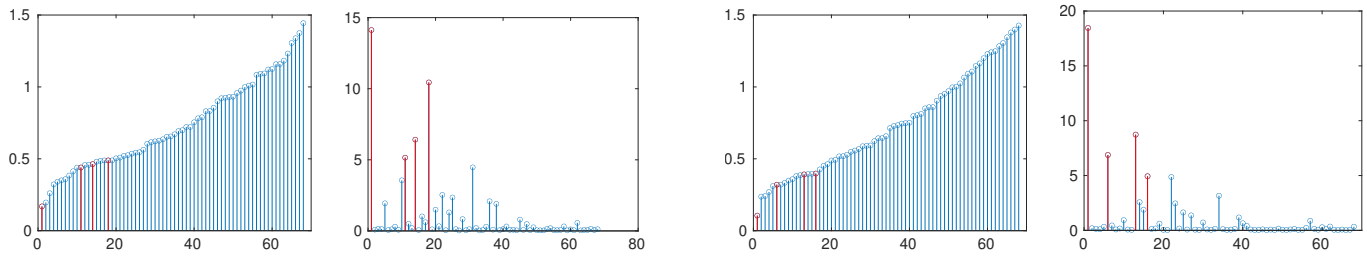

(a) Subject 40. (b) Subject 70.

Fig. 2. Joint eigenvalues for different representative subjects from dataset [15]. Notice that there is no consistent ordering in the dominant eigenmodes with reference to ascending ordering of joint Laplacian eigenvlaues ($\boldsymbol{\Phi}$).

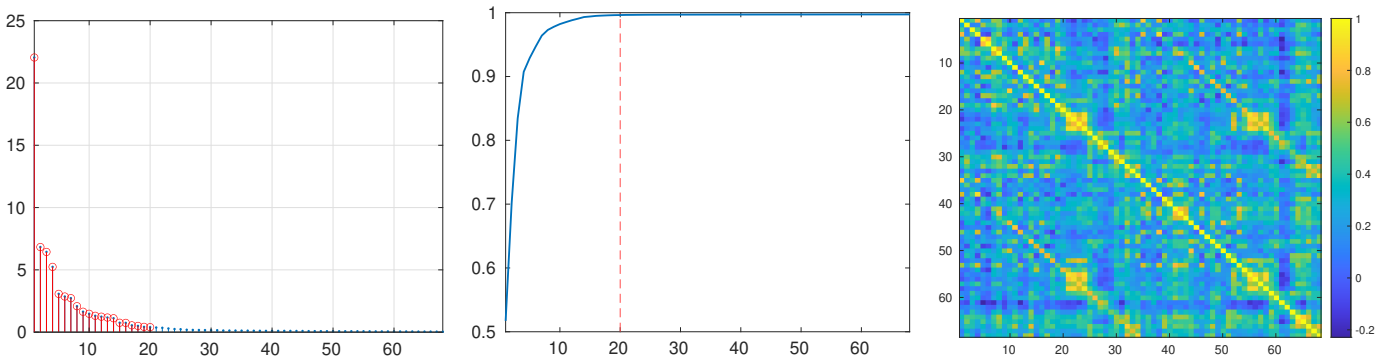

(a) Ψ. (b) Pearson R plot. (c) Ground-truth $\boldsymbol{F}$.

Brain atlas of size (68×68).

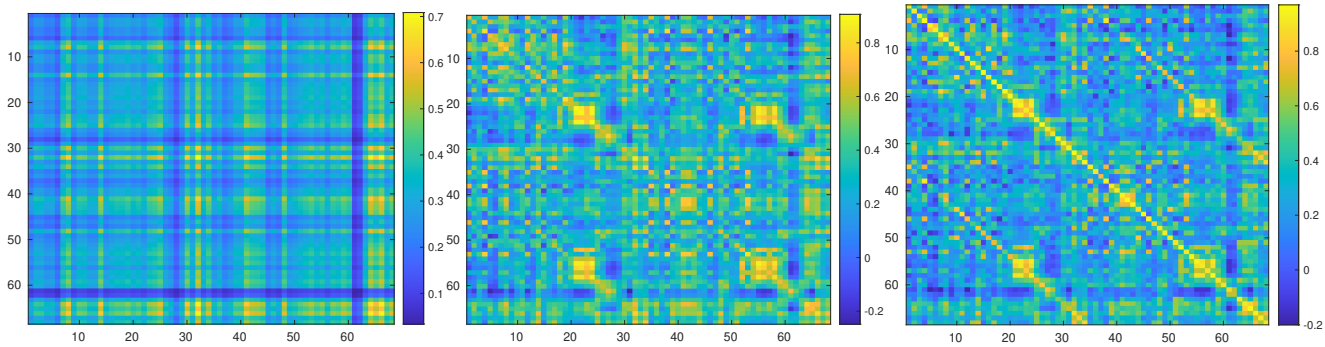

(d) $K = 1$. (e) $K = 5$. (f) Estimated $\boldsymbol{F}$ (top 20 modes).

Atlas (68×68): Progression of estimated FC vs K.

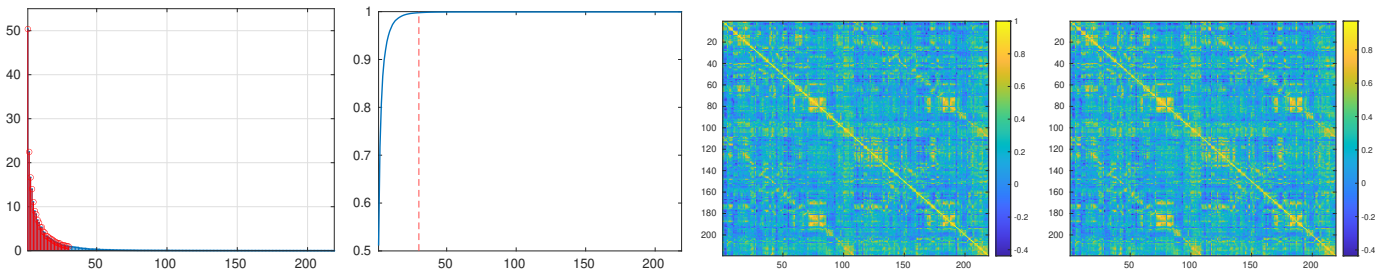

(g) Ψ. (h) Pearson R plot. (i) Ground-truth $\boldsymbol{F}$. (j) Estimated $\boldsymbol{F}$ (top 30 modes).

Brain atlas of size (219×219).

Fig. 3. Example of subspace relationship in structure-function joint eigen-spectrum. (a): $\boldsymbol{\Psi}$ obtained via joint diagonalization. Top K = 20 values are marked in red. (b): Plot of Pearson R value as a function of $\boldsymbol{K}$. For each $\boldsymbol{K}$, we estimate functional connectome as in (II). The red dotted x-line indicates the instance when estimated functional connectome almost matches with the ground-truth one. In the top example, it is $\boldsymbol{K = 20}$ where the Pearson R is $\mathbf{0.996}$. Similarly, for $\boldsymbol{K = 30}$, the Pearson R is $\mathbf{0.998}$ in case of $(\mathbf{219} \times \mathbf{219})$ atlas in the buttom example. The respective estimated functional connectomes are displayed in the last column. It is evident that both the estimated connectomes are visually indistinguishable to the true functional connectomes shown in third column. These examples demonstrate that functional connectome lies within structural connectome.

connectome of the subject. Following [19], the functional eigenspectra Γ were estimated using an exponential transformation of Λ.

2) Tewarie et al. [14]: We implemented the optimization framework of [14] to estimate the projections of functional connectome on the eigenmodes of structural connectome.
3) Becker et al. [13]: We implemented the stucture-function mapping method in [13], where given both structural and functional connectomes of a particular subject, a rotation matrix and a polynomial expansion of the respective eigenspectra were used to estimate the functional connectome from structure.

C. Performance Evaluation of the Predictive Model

We study the effectiveness of the proposed method in terms of accurately estimating functional connectome (FC) of a subject from its structural connectome (or Laplacian) and compare with state-of-the-art methods in the literature. The prediction performance is quantified in terms of Pearson R statistic between the estimated FC and true FC of a subject.

In our group level prediction pipeline, we learn the mapping between joint eigenvalues of structural Laplacian and eigenvalues of functional connectome. First, we use both connectomes of the entire set of subjects. Next we learn group level joint eigenmodes by solving an optimization problem using the toolbox in [27]. Both the mapping and joint eigenmodes are further refined through few iterations. Finally, we use the learned mapping and group level joint modes to predict functional connectome of a subject from structural connectivity.

IV. Results

In this section, we perform exhaustive experiments to examine the effectiveness of the proposed joint eigenmode approach in structure-function mapping. We start with detailed experimentation of our proposed eigenspectrum mapping approaches. Finally, we compare with state-of-the-art methods in the literature for structure-function mapping.

In Figures 4 and 5, we present visual results of estimated functional connectomes using our method for two representative subjects [15]. We display the results using the benchmark methods: Abdelnour et al. [12], Tewarie et al. [14], and Becker et al. [13]. The respective Pearson R values are noted below each panel. It is visually evident that proposed JESM outperforms both Abdelnour et al. [12] and Tewarie et al. [14] by a significant margin. The estimated functional using JESM more closely resembles the ground-truth as compared to the ones produced by Becker et al. [13].

We summarize the comparison of our proposed algorithm and benchmarks for structure function prediction using violin plots in Figure 6. A total 70 healthy subjects from the dataset [15] were used to learn the proposed eigen mapping operator W and joint eigenmodes $\mathcal{A}$. For all algorithms, we compute Pearson R for all the subjects and displayed in violin plots. We note that the proposed JESM method outperforms the benchmarks by a significant margin.

V. Discussion

We provided a principled mathematical framework to connect the structural and functional connectivity matrices. By expressing both connectomes using a common eigen space, we simplified subspace relationship between structural and functional connectomes. We mathematically validated a fundamental hypothesis in neuroscience that structural connections imply functional ones [1], [28]. We developed a novel algorithm for predicting functional connectomes based on structural connectomes and joint mapping, and demonstrate the superiority of this prediction algorithm compared to existing benchmarks.

The existence of joint subspace between structural Laplacian and functional connectome for a particular subject provides a new insight towards understanding the relationship between them. In particular, the results in Fig. 3 suggest that only a few number of joint eigenmodes are sufficient to approximate the functional connectome. From theoretical point of view, this is a remarkable result. It is noteworthy that the joint eigenvalues of functional connectome are sparse in nature; only very few are significant, reflecting the low-rank property of functional connectome. The joint subspace enables the projection of functional time-series onto a common structure-function manifold that is preserved across subjects.

The group level predictive model is of particular interest to us. We note that there is no direct connection between joint eigenmodes across subjects. Therefore, for predicting the functional connectome for a particular subject from its structural connnectome via joint subspace mapping, we need to know: (i) the mapping between joint eigenspectra of both and (ii) joint eigenmodes which closely diagonalize both connectomes. We address this concern by two-step optimization. First, we learn a mapping from joint eigenvalues of structural Laplacian to joint eigenvalues of functional connectome via spectrum mapping. Second, we use this learned spectrum mapping to estimate a joint eigenmodes using manifold optimization. By efficient use of advanced numerical optimization, we obtain a group level eigenmodes that jointly diagnolize individual subject level structural and functional connectomes.

Among the notable existing works, [12] predicts the functional connectome using the eigenmodes of structural Laplacian. Authors in [14] formulated this structure function mapping as a L_2 minimization problem where the feasible eigenmodes were restricted to the individual eigenmodes of structural connectome. Becker et al. [13] proposed an efficient eigenmode mapping, by introducing a rotation matrix along with the structural eigenmodes as a means to capture individual subjects' FC. However, our approach is quite different from [13] in terms of the mathematical formulations: (i) we do not assume any direct relationship between the connectomes, rather we just estimate joint eigenmodes between them, (ii) we consider a more simpler linear mapping between eigenspectra than rotation operators of eigenspectra.

Finally, although we focus here on joint eigenmodes and eigenspectra between the structural Laplacian and functional connectomes obtained from fMRI, our approach is general and applicable to functional connectomes obtained from other

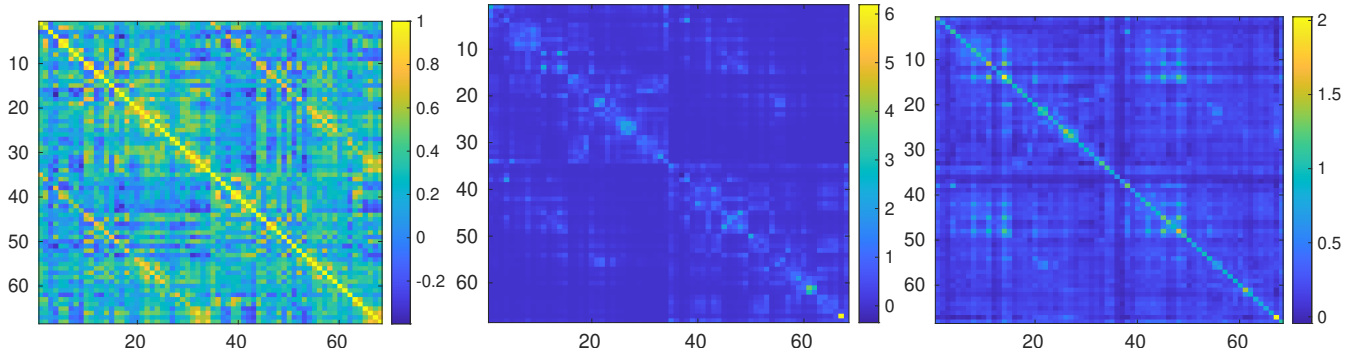

(a) Ground-truth. (b) Abdelnour, R = 0.253. (c) Tewarie, R = 0.247.

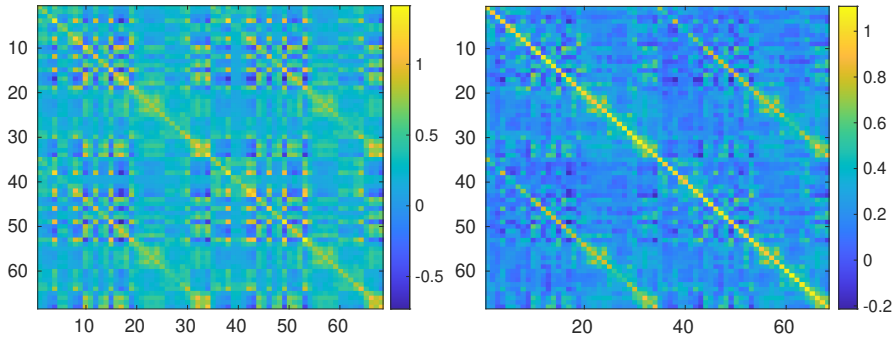

(d) Becker, R = 0.626. (e) JESM, R = 0.746.

Fig. 4. Visual comparison of structure function mapping on Subject 43. The Pearson R values are reported in the sub-captions. A higher R value indicates superior prediction. Among all the methods, our proposed method JESM achieves best results in terms of both visual quality and R value.

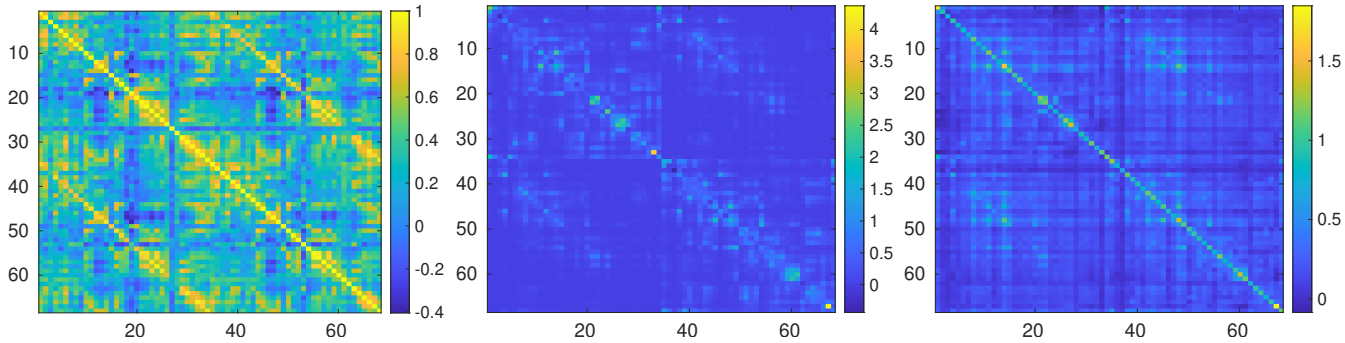

(a) Ground-truth. (b) Abdelnour, R = 0.229. (c) Tewarie, R = 0.129.

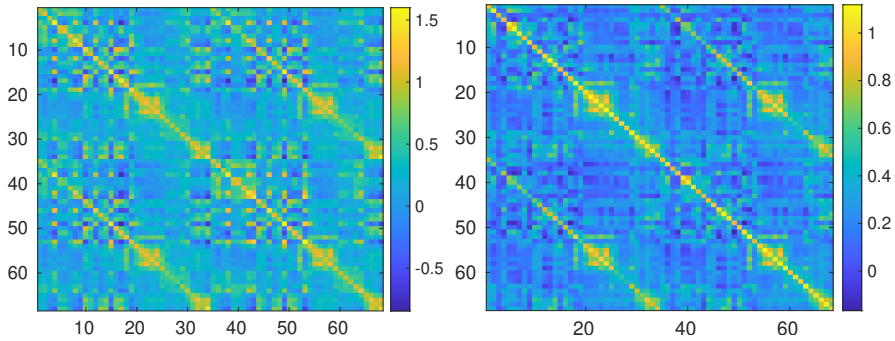

(d) Becker, R = 0.594. (e) JESM, R = 0.661.

Fig. 5. Visual comparison of structure function mapping on Subject 58. The Pearson values are also reported in the sub-captions. A higher R value indicates superior prediction. Our proposed method JESM achieves best results in terms of both visual quality and Pearson R value.

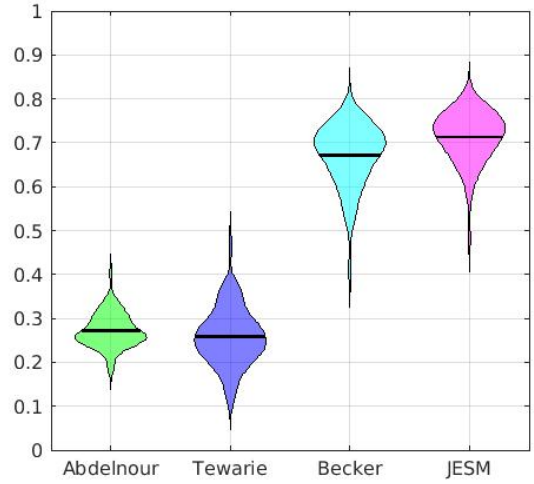

Fig. 6. Violin plot of Pearson R value on the entire set of subjects. Notice that our proposed method joint eigen spectrum mapping (JESM) outperforms the existing state-of-the-art approaches.

TABLE I

SUMMARY OF THE VARIABLES AND DEFINITIONS USED IN THIS TEXT.

Symbol	Description
N	Numer of region-of-interest (ROI).
$\boldsymbol{S}$	Structural connectome of size $(N \times N)$.
$\boldsymbol{L}$	Laplacian of structural connectome.
$\boldsymbol{F}$	Functional connectome.
Λ	Eigenvalues of Laplacian ($\boldsymbol{L}$).
U	Eigenvectors of Laplacian.
Γ	Eigenvalues of functional connectome.
V	Eigenvectors of functional connectome.
Φ	Joint eigenvalues of Laplacian ($\boldsymbol{L}$).
Ψ	Joint eigenvalues of functional connectome ($\boldsymbol{F}$).
$\mathcal{A}$	Joint eigenmodes of $\boldsymbol{L}$ and $\boldsymbol{F}$.
M	Number of subjects.
$\boldsymbol{L}_j$	Laplacian of subject j.
$\boldsymbol{F}_j$	Functional connectome of subject j.
Φ_j	Joint eigenvalues of Laplacian of subject j.
Ψ_j	Joint eigenvalues of functional connectome of subject j.
Δ_Λ	Diagonal matrix with diagonal entries Λ.
Δ_Γ	Diagonal matrix with diagonal entries Γ.
Δ_Φ	Diagonal matrix with diagonal entries Φ.
Δ_Ψ	Diagonal matrix with diagonal entries Ψ.
Δ_{Φ_j}	Diagonal matrix with diagonal entries Φ_j of subject j.
Δ_{Ψ_j}	Diagonal matrix with diagonal entries Ψ_j of subject j.

functional neuroimaging methods like MEG and EEG. A more general extension of the problem of joint mapping posed here is the examination of joint functional and structural eigenmodes across multiple functional connectomes obtained either from multiple modalities or from dynamic functional connectivity methods. Our long-term vision is to obtain potentially sensitive structure-function biomarkers for differential diagnosis or prognosis or therapeutic monitoring in various neurological disorders.

APPENDIX

Lemma 1: For any $\boldsymbol{x} \in \mathbb{R}^{N\times 1}$ spanned by joint eigenvectors, the maximum joint eigenvalue of structural Laplacian follows

$$\max_{\boldsymbol{x}} \frac{\boldsymbol{x}^T \boldsymbol{L}\boldsymbol{x}}{\boldsymbol{x}^T\boldsymbol{x}} = \phi_N. \tag{10}$$

Proof: We have $\boldsymbol{a}_i, i \in \{1, 2, \ldots, N\}$ be joint eigenvectors in $\mathcal{A}$ such that $\boldsymbol{a}_N$ is the eigenvector corresponding to the largest joint eigenvalue ϕ_N and $\boldsymbol{a}_1$ is the joint eigenmode corresponds to the smallest joint eigenvalue ϕ_1. Suppose $x = (c_1\boldsymbol{a}_1 + c_2\boldsymbol{a}_2 + \ldots + c_N\boldsymbol{a}_N)$, for some constants $\{c_1, c_2, \ldots, c_N\}$. Then

$$\boldsymbol{x}^T\boldsymbol{L}\boldsymbol{x} = (c_1\boldsymbol{a}_1 + \ldots + c_N\boldsymbol{a}_N)^T\boldsymbol{L}(c_1\boldsymbol{a}_1 + \ldots + c_N\boldsymbol{a}_N).$$

Using the properties of joint eigenmodes $\boldsymbol{L}\boldsymbol{a}_i = \phi_i\boldsymbol{a}_i$ for $i \in \{1, 2, \ldots, N\}$, we get

$$\begin{aligned}\boldsymbol{x}^T\boldsymbol{L}\boldsymbol{x} &= (c_1\boldsymbol{a}_1 + \ldots + c_N\boldsymbol{a}_N)^T(c_1\phi_1\boldsymbol{a}_1 + \ldots + c_N\phi_N\boldsymbol{a}_N)\\ &= \sum_{i=1}^{N} c_i^2\phi_i. \quad (\text{since } \boldsymbol{a}_1, \boldsymbol{a}_2, \ldots, \boldsymbol{a}_N \text{ are orthonormal})\end{aligned}$$

Similarly, $\boldsymbol{x}^T\boldsymbol{x} = \sum_{i=1}^N c_i^2$. Therefore,

$$\frac{\boldsymbol{x}^T\boldsymbol{L}\boldsymbol{x}}{\boldsymbol{x}^T\boldsymbol{x}} = \frac{\sum_{i=1}^N c_i^2\phi_i}{\sum_{i=1}^N c_i^2} \leq \frac{\phi_N \sum_{i=1}^N c_i^2}{\sum_{i=1}^N c_i^2} = \phi_N. \qquad \blacksquare$$

Lemma 2: Given a symmetric matrix S with non-negative entries, and its diagonal degree matrix D, and the matrix $\tilde{\boldsymbol{S}} = \boldsymbol{D}^{-1/2}\boldsymbol{S}\boldsymbol{D}^{-1/2}$, then both $(\boldsymbol{I} - \tilde{\boldsymbol{S}})$ and $(\boldsymbol{I} + \tilde{\boldsymbol{S}})$ are positive semi-definite (PSD) matrices.

Proof: For any given $\boldsymbol{x} \in \mathbb{R}^N$, spanned the joint eigenvectors in $\mathcal{A}$ we can write:

$$\boldsymbol{x}^T(\boldsymbol{D} - \boldsymbol{S})\boldsymbol{x} = \sum_{(i,j),(i\neq j)} S_{ij}(x_i - x_j)^2, \tag{11}$$

where $S_{ij} = S_{ji}$ using the symmetric properties of $\boldsymbol{S}$. By construction of structural connectivity, each entry of S is non-negative real number. Therefore

$$\boldsymbol{x}^T(\boldsymbol{D} - \boldsymbol{S})\boldsymbol{x} \geq 0.$$

This proves that $(\boldsymbol{D} - \boldsymbol{S})$ is a positive semi-definite matrix: $(\boldsymbol{D} - \boldsymbol{S}) \succcurlyeq 0$. We use the properties of eigenvalues of multiplication of matrices [29]. Since $\boldsymbol{D}$ is positive definite matrix, $\boldsymbol{D}^{-1/2}$ is also positive definite. Therefore

$$\boldsymbol{D}^{-1/2}(\boldsymbol{D} - \boldsymbol{S})\boldsymbol{D}^{-1/2} = (\boldsymbol{I} - \tilde{\boldsymbol{S}}) \succcurlyeq 0. \tag{12}$$

Similar to (11), we have

$$\boldsymbol{x}^T(\boldsymbol{D} + \boldsymbol{S})\boldsymbol{x} = \sum_{(i,j),(i\neq j)} S_{ij}(x_i + x_j)^2 \geq 0. \tag{13}$$

Using the properties of eigenvalues of matrix multiplication,

$$\boldsymbol{D}^{-1/2}(\boldsymbol{D} + \boldsymbol{S})\boldsymbol{D}^{-1/2} = (\boldsymbol{I} + \tilde{\boldsymbol{S}}) \succcurlyeq 0. \tag{14}$$

A. Proof of Theorem 1

The lower bound on eigenvalues of $\boldsymbol{L}$ directly follows from (12) in Lemma 2. It proves that $\boldsymbol{L} = (\boldsymbol{I} - \tilde{\boldsymbol{S}})$ is a PSD matrix. Therefore, the minimum joint eigenvalue of $\boldsymbol{L}$ follows $\phi_1 \geq 0$.

To show the upper bound of eigenvalues of $\boldsymbol{L}$, we recall (14) in Lemma 2 that $(\boldsymbol{I} + \tilde{\boldsymbol{S}}) \succcurlyeq 0$. For any x, spanned the joint eigenvectors in $\mathcal{A}$, we have

$$\boldsymbol{x}^T\boldsymbol{x} + \boldsymbol{x}^T\tilde{\boldsymbol{S}}\boldsymbol{x} \geq 0 \implies \boldsymbol{x}^T\boldsymbol{x} \geq -\boldsymbol{x}^T\tilde{\boldsymbol{S}}x.$$

By adding a positive quantity $\boldsymbol{x}^T\boldsymbol{x}$ to both sides:

$$\boldsymbol{x}^T\boldsymbol{x} - \boldsymbol{x}^T\tilde{\boldsymbol{S}}x \leq 2\boldsymbol{x}^T\boldsymbol{x} \implies \boldsymbol{x}^T(\boldsymbol{I} - \tilde{\boldsymbol{S}})\boldsymbol{x} \leq 2\boldsymbol{x}^T\boldsymbol{x}.$$

By further simplification,

$$\frac{\boldsymbol{x}^T \boldsymbol{L} \boldsymbol{x}}{\boldsymbol{x}^T \boldsymbol{x}} \leq 2. \tag{15}$$

Combining (10) in Lemma 1 and (15), we obtain $\phi_N \leq 2$. ■

B. Proof of Theorem 2

We show here that each functional connectome is a positive semi-definite matrix. Without loss of generality, we note that functional connectome [26], [30] basically measures the second moment matrix of a temporal signal (/random variable) $\boldsymbol{z} \in \mathbb{R}^{N \times 1}$. In particular,

$$\boldsymbol{F} = E(\boldsymbol{z}\boldsymbol{z}^T).$$

Suppose there are T time-point at each ROI is used to estimate the connectivity. Then, $E(\boldsymbol{z}\boldsymbol{z}^T) = \frac{1}{T}\sum_{t=1}^{T} \boldsymbol{z}(t)\boldsymbol{z}(t)^T$. Now, for any random vector $\boldsymbol{b} \in \mathbb{R}^{N \times 1}$, we can write

$$\boldsymbol{b}^T \boldsymbol{F} \boldsymbol{b} = \boldsymbol{b}^T E(\boldsymbol{z}\boldsymbol{z}^T)\boldsymbol{b} = E(\boldsymbol{b}^T \boldsymbol{z}\boldsymbol{z}^T \boldsymbol{b}) = E\big((\boldsymbol{b}^T \boldsymbol{z})^2\big) \geq 0.$$

Note that $\boldsymbol{b}^T \boldsymbol{F} \boldsymbol{b}$ is the expectation of the square of the scalar random variable $\hat{z} = \boldsymbol{b}^T \boldsymbol{z}$. Therefore, for any eigenvectors in $\mathcal{A}$, the respective eigenvalue is non-negative. ■

References

[1] Gustavo Deco, Viktor K Jirsa, and Anthony R McIntosh, "Emerging concepts for the dynamical organization of resting-state activity in the brain," *Nature Reviews Neuroscience*, vol. 12, no. 1, pp. 43–56, 2011.

[2] Selen Atasoy, Isaac Donnelly, and Joel Pearson, "Human brain networks function in connectome-specific harmonic waves," *Nature Communications*, vol. 7, no. 1, pp. 1–10, 2016.

[3] Peter A Robinson, "Interrelating anatomical, effective, and functional brain connectivity using propagators and neural field theory," *Physical Review E*, vol. 85, no. 1, pp. 011912, 2012.

[4] Maria Luisa Saggio, Petra Ritter, and Viktor K Jirsa, "Analytical operations relate structural and functional connectivity in the brain," *PloS one*, vol. 11, no. 8, pp. e0157292, 2016.

[5] Jil Meier, Prejaas Tewarie, Arjan Hillebrand, Linda Douw, Bob W van Dijk, Steven M Stufflebeam, and Piet Van Mieghem, "A mapping between structural and functional brain networks," *Brain Connectivity*, vol. 6, no. 4, pp. 298–311, 2016.

[6] Gideon Rosenthal, Frantisek Vasa, Alessandra Griffa, Patric Hagmann, Enrico Amico, Joaquín Goñi, Galia Avidan, and Olaf Sporns, "Mapping higher-order relations between brain structure and function with embedded vector representations of connectomes," *Nature communications*, vol. 9, no. 1, pp. 1–12, 2018.

[7] Raphael Liégeois, Augusto Santos, Vincenzo Matta, Dimitri Van De Ville, and Ali H Sayed, "Revisiting correlation-based functional connectivity and its relationship with structural connectivity," *Network Neuroscience*, vol. 4, no. 4, pp. 1235–1251, 2020.

[8] David Pascucci, Maria Rubega, Joan Rué-Queralt, Sebastien Tourbier, Patric Hagmann, and Gijs Plomp, "Structure supports function: informing directed and dynamic functional connectivity with anatomical priors," *bioRxiv*, 2021.

[9] Arnaud Messé, Habib Benali, and Guillaume Marrelec, "Relating structural and functional connectivity in MRI: A simple model for a complex brain," *IEEE Transactions on Medical Imaging*, vol. 34, no. 1, pp. 27–37, 2014.

[10] Arnaud Messé, Marc-Thorsten Hütt, Peter König, and Claus C Hilgetag, "A closer look at the apparent correlation of structural and functional connectivity in excitable neural networks," *Scientific Reports*, vol. 5, no. 1, pp. 1–5, 2015.

[11] Fani Deligianni, Gaël Varoquaux, Bertrand Thirion, David J Sharp, Christian Ledig, Robert Leech, and Daniel Rueckert, "A framework for inter-subject prediction of functional connectivity from structural networks," *IEEE Transactions on Medical Imaging*, vol. 32, no. 12, pp. 2200–2214, 2013.

[12] Farras Abdelnour, Michael Dayan, Orrin Devinsky, Thomas Thesen, and Ashish Raj, "Functional brain connectivity is predictable from anatomic network's Laplacian eigen-structure," *NeuroImage*, vol. 172, pp. 728–739, 2018.

[13] Cassiano O Becker, Sérgio Pequito, George J Pappas, Michael B Miller, Scott T Grafton, Danielle S Bassett, and Victor M Preciado, "Spectral mapping of brain functional connectivity from diffusion imaging," *Scientific Reports*, vol. 8, no. 1, pp. 1–15, 2018.

[14] Prejaas Tewarie, Bastian Prasse, Jil M Meier, Fernando AN Santos, Linda Douw, Menno M Schoonheim, Cornelis J Stam, Piet Van Mieghem, and Arjan Hillebrand, "Mapping functional brain networks from the structural connectome: Relating the series expansion and eigenmode approaches," *NeuroImage*, vol. 216, pp. 116805, 2020.

[15] A Griffa, Y Alemán-Gómez, and P Hagmann, "Structural and functional connectome from 70 young healthy adults [data set]," *Zenodo*, 2019.

[16] Jean-François Cardoso and Antoine Souloumiac, "Jacobi angles for simultaneous diagonalization," *SIAM Journal on Matrix Analysis and Applications*, vol. 17, no. 1, pp. 161–164, 1996.

[17] Xavier Luciani and Laurent Albera, "Joint eigenvalue decomposition of non-defective matrices based on the LU factorization with application to ICA," *IEEE Transactions on Signal Processing*, vol. 63, no. 17, pp. 4594–4608, 2015.

[18] Rémi André, Xavier Luciani, and Eric Moreau, "Joint eigenvalue decomposition algorithms based on first-order Taylor expansion," *IEEE Transactions on Signal Processing*, vol. 68, pp. 1716–1727, 2020.

[19] Farras Abdelnour, Henning U Voss, and Ashish Raj, "Network diffusion accurately models the relationship between structural and functional brain connectivity networks," *Neuroimage*, vol. 90, pp. 335–347, 2014.

[20] Sanjay Ghosh and Kunal N Chaudhury, "On fast bilateral filtering using Fourier kernels," *IEEE Signal Processing Letters*, vol. 23, no. 5, pp. 570–573, 2016.

[21] Ting Kei Pong, Paul Tseng, Shuiwang Ji, and Jieping Ye, "Trace norm regularization: Reformulations, algorithms, and multi-task learning," *SIAM Journal on Optimization*, vol. 20, no. 6, pp. 3465–3489, 2010.

[22] Zhang Liu and Lieven Vandenberghe, "Interior-point method for nuclear norm approximation with application to system identification," *SIAM Journal on Matrix Analysis and Applications*, vol. 31, no. 3, pp. 1235–1256, 2010.

[23] P-A Absil, Robert Mahony, and Rodolphe Sepulchre, *Optimization algorithms on matrix manifolds*, Princeton University Press, 2009.

[24] Alessandro Daducci, Stephan Gerhard, Alessandra Griffa, Alia Lemkaddem, Leila Cammoun, Xavier Gigandet, Reto Meuli, Patric Hagmann, and Jean-Philippe Thiran, "The connectome mapper: an open-source processing pipeline to map connectomes with MRI," *PloS one*, vol. 7, no. 12, pp. e48121, 2012.

[25] Van J Wedeen, RP Wang, Jeremy D Schmahmann, Thomas Benner, Wen-Yih Isaac Tseng, Guangping Dai, DN Pandya, Patric Hagmann, Helen D'Arceuil, and Alex J de Crespigny, "Diffusion spectrum magnetic resonance imaging (DSI) tractography of crossing fibers," *Neuroimage*, vol. 41, no. 4, pp. 1267–1277, 2008.

[26] Jonathan D Power, Kelly A Barnes, Abraham Z Snyder, Bradley L Schlaggar, and Steven E Petersen, "Spurious but systematic correlations in functional connectivity mri networks arise from subject motion," *Neuroimage*, vol. 59, no. 3, pp. 2142–2154, 2012.

[27] Nicolas Boumal, Bamdev Mishra, P-A Absil, and Rodolphe Sepulchre, "Manopt, a Matlab toolbox for optimization on manifolds," *The Journal of Machine Learning Research*, vol. 15, no. 1, pp. 1455–1459, 2014.

[28] Marco Aqil, Selen Atasoy, Morten L Kringelbach, and Rikkert Hindriks, "Graph neural fields: a framework for spatiotemporal dynamical models on the human connectome," *PLoS Computational Biology*, vol. 17, no. 1, pp. e1008310, 2021.

[29] AR Meenakshi and C Rajian, "On a product of positive semidefinite matrices," *Linear Algebra and Its Applications*, vol. 295, no. 1-3, pp. 3–6, 1999.

[30] Jose M Sanchez Bornot, KongFatt Wong-Lin, Alwani Liyana Ahmad, and Girijesh Prasad, "Robust eeg/meg based functional connectivity with the envelope of the imaginary coherence: sensor space analysis," *Brain Topography*, vol. 31, no. 6, pp. 895–916, 2018.